Improved urban canopy model for building energy simulation with ray tracing

Léo Bourquin, Mathias Bouquerel, Thierry Duforestel, Sébastien Bermes, Emmanuel Bozonnet

Improved urban canopy model for building energy simulation with ray tracing

Léo Bourquin[1,2,4], Mathias Bouquerel[1,4], Thierry Duforestel[1,4], Sébastien Bermes[5], Emmanuel Bozonnet[2,3,4]
[1]EDF R&D, Moret-Loing-et-Orvanne, France
[2]LaSIE UMR CNRS 7356, La Rochelle, France
[3]IRSTV FR CNRS 2488, Nantes, France
[4]Laboratoire Commun 4eV Lab EDF & LaSIE, France
[5]EnerBIM, Donneville, France

Abstract

The urban heat island (UHI) affects energy consumption as well as heating and cooling demand in cities. Traditional urban canopy models, such as the Urban Weather Generator (UWG), can be used to estimate the impact of the UHI on the outdoor air temperature. They simplify urban morphology by assuming idealized averaged street canyons. This limits the accuracy of solar radiation modeling, a critical component of urban energy balance. To address this, we propose integrating detailed ray tracing solar calculations into UWG, leveraging Building Information Models (BIM) to enhance geometric precision. A case study on a real neighborhood shows the impact on shortwave irradiance and air temperature predictions, with measurable but limited impacts on cooling demand.

Key Innovations

- Integration of detailed ray tracing solar calculations into the Urban Weather Generator (UWG) framework, replacing simplified urban canyon assumptions
- A novel methodology for coupling BIM-based geometry with urban canopy models, paving the way for more precise microclimate and energy assessments

Practical Implications

Improving solar gain modeling in the urban canopy layer can reduce inaccuracies in the urban air temperature prediction, and thus improve the energy demand predictions.

1 Introduction

The urban heat island (UHI) is a widely studied phenomenon that amplifies air temperatures in cities compared to their rural surroundings (Oke, 1987). Urbanization alters the diurnal cycle of air temperature through increased effective albedo, reduced wind speeds, and limited evaporative cooling due to reduced vegetative surfaces. Considering that buildings account for about 40% of primary global energy consumption (Santamouris 2014; Pérez-Lombard, Ortiz, et Pout 2008), UHI effect significantly impacts both total energy consumption and peak power demand by strongly altering building energy needs (Bueno et al. 2012; Bozonnet, 2005).

Urban canopy models such as the model implemented in Urban Weather Generator (UWG) (Bruno Bueno et al. 2013) simplify the urban morphology. While this approach is sufficient for many urban climate studies, it introduces inaccuracies in solar radiation modeling – a key component of the urban energy balance. Solar radiation can contribute up to 50% of the total energy balance in urban areas, underscoring the importance of precise shortwave calculations to improve air temperature predictions, and thus building energy demand predictions (Oke, 1987).

Usually, within urban canopy models like UWG, the solar calculation method assumes a typical street canyon with no specific orientations and solar radiations are averaged over all orientations. In this study, we present a methodology for integrating detailed ray tracing solar calculations into UWG, leveraging BIM (Building Information Model) data to account for complex urban geometries. The proposed approach is tested for a real neighborhood in France, quantifying its impact on solar irradiance, air temperature predictions, and building cooling demands in summer. This work highlights the value of improved radiative modeling in capturing urban heterogeneities and its implications on outdoor air temperature prediction.

2 Method

The aim of this study is to quantify the influence of the urban canopy layer (UCL) modeling, including a detailed solar irradiance modeling, on the urban air temperature, and the energy cooling demand, for a set of Building Energy Models (BEM). This section describes the numerical tools and the coupling approach.

2.1 MyBEM and Building Energy Model

To calculate the building energy demand of the neighborhood, we use **MyBEM**, a modular platform dedicated to building energy modeling (Bouquerel et al. 2021) comprising three main software tools: HelioBIM, Pyrosette, and BuildSysPro.

HelioBIM is used to generate a gbXML (energy oriented BIM file) containing the building data (Bouquerel et al. 2021): the imported 3D geometry, the envelope property that can be edited (construction

 https://doi.org/10.26868/25222708.2025.1153

material and windows properties), and the building operation scenarios. It also features a ray-tracing solar calculation module that calculates hourly solar irradiances (W/m²) for all urban surfaces (see next chapter for more details). **Pyrosette** is a Python package that uses BIM data given by HelioBIM (gbXML and weather data) to generate a BEM. It is designed to instantiate each building component as a Modelica model: each building component described in the BIM has a corresponding model in **BuildSysPro**. BuildSysPro is a free and open-source Modelica library developed by EDF R&D for 0D/1D building energy and system modeling (Plessis, Kaemmerlen, et Lindsay 2014). The approach to building modeling in BuildSysPro aligns with methods widely used by the building science community, where weather data are used as boundary conditions and thus with a single outdoor temperature (T_{rural}). However solar calculations used as boundary conditions in the model generated by PyRosette are performed with HelioBIM. In Figure 1 we propose a simplified diagram of MyBEM.

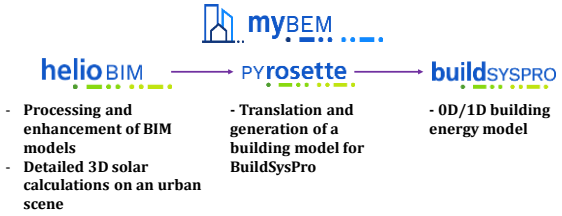

Figure 1: Simplified diagram of MyBEM tool chain.

2.2 HelioBIM Ray tracing method

Computing irradiance on a surface involves summing three components: direct irradiance from the sun (E_b), diffuse irradiance from the sky (E_d), and reflected irradiance from surrounding surfaces (E_r). In Figure 2 we propose a simplified scheme of the method.

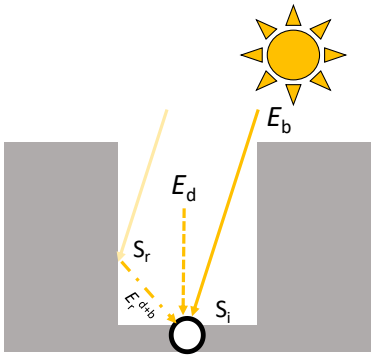

Figure 2: HelioBIM solar calculations scheme.

A commonly used method to calculate these components is Monte Carlo ray tracing, which is implemented in HelioBIM. In this tool, the irradiance is obtained by tracing rays backward, starting from the surface of interest and traveling toward the radiation sources: the sun or the sky.

Direct irradiance is first calculated by casting rays toward the sun from different points of the surface of interest S_i. The proportion of rays that are not intercepted by another surface and the inclination of the surface are used to calculate the direct irradiance.

A set of rays with random directions is then cast from the surface S_i and for each ray, the following steps are performed:

1. Intersection Check:
   - If the ray does not intersect any object, it collects energy directly from the sky, contributing to the diffuse irradiance.
   - If the ray intersects an object, the energy received by that surface S_r is computed.
2. Energy Calculation on surface Sr:
   - Direct Irradiance (E_b): A ray is cast toward the sun. If the sun is unobstructed, its energy contributes directly to the irradiance.
   - Indirect Irradiance (E_r): To account for reflected energy, another ray is recursively cast in a random direction, simulating ray reflections from nearby surfaces. For transmissive surfaces, the transmission ratio is used as the probability of casting the recursive ray through the surface.

To ensure the accuracy of the method, error calculation is used to monitor convergence and control the precision of the results. By summing the contributions from a large number of rays and adjusting for error, the total irradiance on the surface can be determined reliably.
To optimize computational costs, the Monte Carlo algorithm is executed only for a set of carefully selected key positions of the sun (each hour for one day per month). The view factors calculation allows then to express irradiances from E_d and E_b. These view factors are interpolated in order to get values for each hour of the year.

2.3 Microclimate Model

To observe the effect of UHI on the air temperature and then on energy demands, we use the Urban Weather Generator (UWG), an urban mesoscale model widely recognized within the scientific community (Bruno Bueno et al. 2013). It generates an urban air temperature scenario from a rural weather data set. To do so, the rural temperature is passed through a simplified atmospheric model and then through an urban canopy model (UCM), which itself integrates a building energy model to take into account the heat transfer from the building to the air of the urban canopy layer. A coupling mechanism (Bourquin et al. 2024) permits to link HelioBIM with UWG to generate custom building energy models through the automated process of UWG data.

2.4 Presentation of the studied configurations

In this paper, we propose to study how the refinement of the solar radiation modeling in the UCM impacts the urban air temperature ($T_{out,urb}$) and the building energy demand predictions. For this purpose, we consider three

approaches for the Building Energy Model (Table 1): (0) without the UCM, (1) with the UWG model, and (2) with UWG model coupled to a ray tracing model (HelioBIM, (Bouquerel et al. 2021)).

Table 1: Overview diagram of the different software components and configurations of the case study

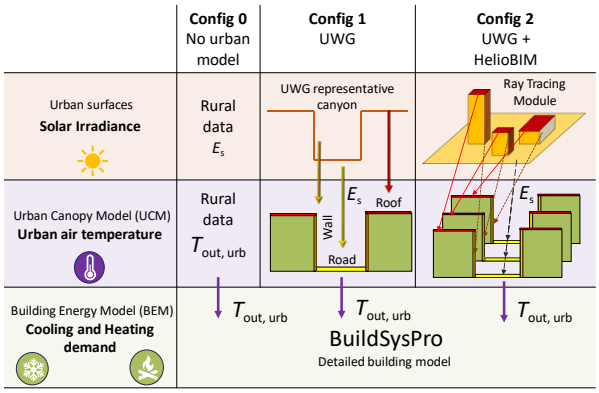

The **Configuration 0** (cf Table 1) is used as reference: the rural weather data (reference weather station) provides the outdoor air temperature used in the Building Energy Model (BuildSysPro).

In the **Configuration 1** (cf Table 1) the outdoor urban air temperature used in the Building Energy Model (BuildSysPro) is calculated with the standard version of UWG. The solar irradiance is computed for an equivalent street canyon, considering the neighborhood morphological data. This is the default radiative model in UWG (Bruno Bueno et al. 2013). All street orientations are equally probable and solar irradiances are averaged and integrated in all directions. The direct, diffuse, and reflected irradiances (E_b, E_d and E_r), expressed in (Masson 2000), are assigned as a single input to all building types in UWG (simplified BEMs), considering an average value for each surface type (walls, roofs, and roads).

In the **Configuration 2** (cf Table 1), the outdoor urban air temperature used in the Building Energy Model (BuildSysPro) is calculated with a version of UWG where the solar irradiance is computed using HelioBIM ray tracing model. Each building in HelioBIM scene is associated with a building type in UWG, with its proportion of presence calculated as the ratio of the building's total surface area to the total surface area of all buildings within the urban zone. Solar inputs for these buildings are derived by averaging HelioBIM's solar data for each surface type, ensuring compatibility with UWG's existing structure. The solar inputs from each building type are then averaged according to their respective proportions to calculate $T_{out,urb}$.

The urban air temperature ($T_{out,urb}$) generated by either of these configurations is used as a boundary condition in the detailed building energy model, i.e. BuildSysPro.

3 Case study presentation

3.1 Location

The first step in our methodology was to select a suitable study area, guided by several criteria:

- High building density and building morphology diversity in order to evaluate the influence of the detailed 3D solar radiation calculations;
- High urban heat island (UHI) risk;
- Far enough from water bodies or large green spaces that could mitigate the UHI;
- Data availability for comparison.

Paris, with its high density and comprehensive data from the PANAME project (PANAME - 2022), met these criteria. PANAME, an experimental collaboration led by Météo-France and other public and private institutions, has provided extensive data since 2022. IoT stations, mounted on the north-facing side of streetlights to avoid direct sunlight exposure, recorded air temperature and relative humidity every 10 minutes. The selected study area is a cluster of buildings along Rivoli Street. For rural comparison, additional data from a station at the edge of Rambouillet Forest were used, capturing air temperature at 10m above ground (PANAME - 2022). In Figure 3, we show the locations of the two measurement sites.

Figure 3: Location of the rural station (green) and the IoT meteorological station (purple)

In this study, we focus exclusively on the summer period, analyzing measurements recorded between July 1, 2022, and September 17, 2022. The UWG model has been calibrated and parameterised for this specific period, but we will show results for the entire summer period from 1st May to 30th September.

3.2 Study area and zones

The neighborhood is modeled with three levels of detail including the following three nested zones, for which the colors (Figure 4) correspond to the modeling scales in Table 1:

- **BEM Zone (Green) :** This zone includes buildings and ground surfaces directly involved in energy balance and solar flux calculations. Each building is treated as an individual simplified building type

https://doi.org/10.26868/25222708.2025.1153

within UWG, and a detailed building in the detailed BuildSysPro BEM. This subset is assumed to be representative of the overall urban area (UCM)

- **Radiation Zone (Orange)**: A bigger area encompassing the BEM zone and additional surrounding buildings. This ensures realistic solar radiation calculations, particularly on building surfaces, used for the UCM in config 2 and for BuildSysPro BEM in all configs.
- **Urban Canopy Model Zone (Purple)**: A 500 m × 300 m area representing the urban canopy layer, used to calculate morphological parameters used in Configuration 1 and 2.

Figure 4: 2D view of the study area and zones. The UCM zone is shown in purple, the radiation zone in orange and the BEM zone in green. In red, the position of the measuring station.

For ground surfaces, the approach mirrors UWG configuration by considering half-street canyons in front of each study building. Full streets are included when study buildings face each other.

3.3 Building properties

Construction materials and windows properties are based on the selected values outlined in the tables below (Table 2 to Table 3). All study buildings are assumed to be Haussmannian-style and non-renovated. (Loga, Stein, et Diefenbach 2016). The fact that no renovation has been applied on buildings is a strong assumption, but then the impact on energy demand will be high and the influence of modeling choices will be easier to observe.

Table 2: Construction material properties

	Composition (exterior to interior)	Width (cm)	Albedo	Thermal resistance (m^2.K/W)
Wall	Cut Stone	50	0.4	**R = 0.32**
	Plasterboard	2.5	.	
Roof	Zinc	0.08	0.6	**R = 0.18**
	Sheathing board	2	.	
	Plasterboard	1.25	.	
Floor	Raw concrete slab	12	.	**R = 0.10**
	Mortar screed	7	.	
Road	Bituminous concrete	4	0.1	**R = 0.34**
	High-modulus asphalt mix	11	.	
	Hydraulic binder materials	27	.	

Table 3: Window properties

	U value ($W/m^2.K$)	SHGC (.)
Window	4.8	0.8

We chose an average glazing ratio of 0.3, which reflects the conditions in the study area, despite being relatively high for non-renovated buildings. Some buildings in the zone have glazing ratios as high as 0.4.

Table 4: Cooling and ventilation scenarios

Cooling	Ventilation
26°C (May 2 to September 30)	0.5 h^{-1}

As one can see, only the cooling setpoint has been configured. As mentioned above, the study will focus solely on the summer period and the cooling demand.

Table 5: Occupancy and Internal Gains scenarios

Occupancy & Internal Gains
Occupancy: 20% (7 AM–6 PM) / 80% (else)
People: 100 W/25 m²
Equipment: 2.5 W/m²

3.4 UWG parameters setting

The study emphasizes accurate determination of two sensitive UWG input parameters: the building density and the vertical-to-horizontal surface ratio. Previous studies have demonstrated that these parameters strongly influence the accuracy of the UCM (Mao et al. 2017; Bruno Bueno et al. 2013). To derive these metrics, we utilized Geoclimate, an open-source toolbox tailored for urban climate research (Bocher et al. 2018). Geoclimate processes high-resolution data from BD TOPO, a French national dataset of land use and topography. While computation time varies with the area size, (Bocher et al. 2021) recommend a minimum zone of 500m to 1km per side for reliable results. From this dataset, we adopt an average building fraction of **0.4** a vertical-to-horizontal surface ratio of **2.16**, given that the UCM zone is relatively homogeneous for these parameters (Figure 4).

4 Results

4.1 Differences on solar irradiances

The first key observation concerns solar irradiances. As noted earlier, each surface of every building has its own specific irradiance. In configuration 2, we calculate an average value for each surface type (wall or roof) of each building. The same process applies to roads. The

https://doi.org/10.26868/25222708.2025.1153

following heatmap (Figure 5) illustrates the hourly (ordinates axe) wall irradiance for two buildings, as calculated by the ray tracing method, compared to the average value used by UWG (configuration 1) and the average for configuration 2.

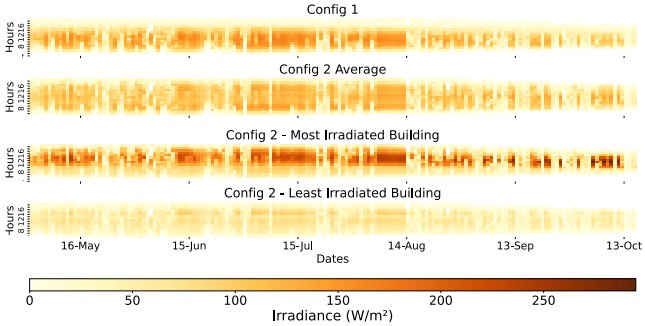

Figure 5: Façade irradiance (W/m2) heatmap for two buildings (config 2), config 1 and average config 2.

As UWG (configuration 1) provides the same irradiance value for all buildings, the irradiance of individual buildings is not shown for this configuration (it will be the same as the average). Furthermore, we have chosen the most and least irradiated buildings, respectively building 2 and building 18.

It reveals noticeable variability in irradiance based on a building's orientation within the selected zone. The most irradiated building (building 18) has a south-facing orientation and receives significantly higher solar flux than Building 2 which is predominantly north-facing.

Figure 6 presents the distribution of wall irradiance values for all buildings over four days in August.

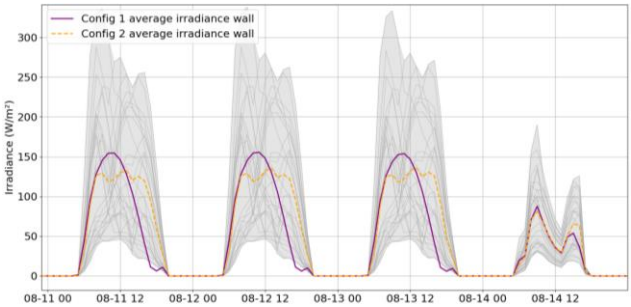

Figure 6: Wall irradiance distribution for all buildings and the average of the two configurations.

The cumulative wall exposure over the whole summer period (1st May – 30th September) is:

- **140 kWh/m²** for Configuration 1
- **151 kWh/m²** for Configuration 2

These results show that the analytical radiative model of UWG (Config 1) slightly underestimates solar irradiances compared to the ray-tracing method implemented in HelioBIM (Config 2). Moreover, irradiance vary considerably based on building orientation (Figure 5). HelioBIM and its ray tracing model allow to simulate the variation of irradiance for individual buildings within the canopy at a low computational cost (less than 2 minutes for a year), however the average differences remain minor.

4.2 Differences on air temperatures

The second key physical parameter to consider is the outdoor air temperature in the canyon. UWG uses a wide range of parameters (over fifty), each having a varying degree of influence on the results. Sensitivity analyses were conducted to identify the most influential parameters on the urban heat island (UHI) effect (Mao et al. 2017; Martinez et al. 2021; Hamdi et al. 2024)

We present below (Figure 7) the root mean square error (RMSE) between the simulated air temperature ($T_{out,urb}$ from Config 1 or Config 2) and the experimental data as a function of the following normalized variation of parameters [0-1] corresponding to the ranges in Table 6:

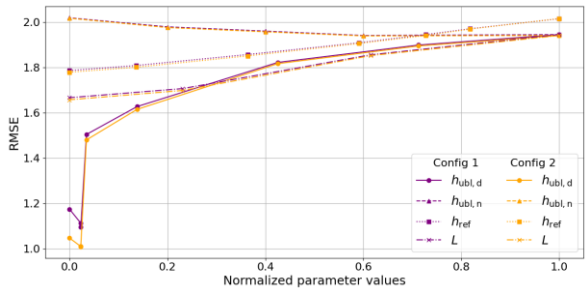

Figure 7: RMSE (°C) as function of normalized UWG parameters

Table 6: Range of variation of UWG parameters

Parameter	min value	max value
$h_{ubl,d}$ (day)	90 m	1000 m
$h_{ubl,n}$ (night)	60 m	80 m
h_{ref}	150 m	85 m
L	1000 m	10200 m

We find in Table 6 the UBL (Urban Boundary Layer) height (h_{UBL}) for day and night (index d and n), the reference height (theoretical height where the potential temperature gradient becomes zero), and the characteristic length L, which represents the theoretical surface of exchange between the city and the sboundary layer.

This RMSE is calculated over the period for which real data is available and on which our study is based, from July 22 to September 17. The most significant parameters for RMSE are the urban boundary layer heights (day: $h_{ubl,d}$ and night: $h_{ubl,n}$) and the reference height, with $h_{ubl,d}$ having the greatest impact.

To minimize the RMSE, the calibrated value of the boundary layer heights is 90 m for daytime and 60 m for nighttime. We obtain:

RMSE Config 1 = ***1.22 °C ;*** *RMSE Config 2 =* ***1.10 °C***

A configuration of atmospheric parameters like the one we chose, with an extremely low daytime boundary

https://doi.org/10.26868/25222708.2025.1153

layer height, results in a daytime urban heat island that is significantly stronger than what UWG is typically able to produce. Indeed, it tends to underestimate the daytime urban heat island and performs better for nocturnal UHI (Hamdi et al. 2024).

This trend is confirmed in Figure 8 which shows the air temperatures for Configurations 1 and 2 for 3 days in August and in Figure 9, with the daily average temperature curves. For the last one, since we represent average daily values, the shaded pink represents the temperature range for config 1 (between a daily min and max value).

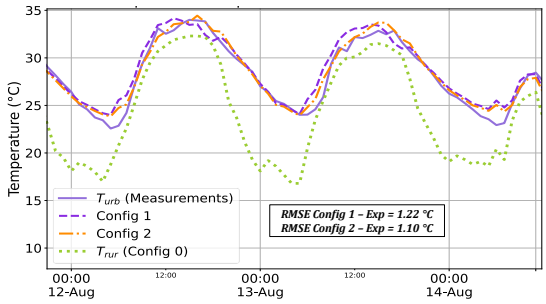

Figure 8 : Comparison of Temperatures: Simulations vs Rivoli data set from PANAME

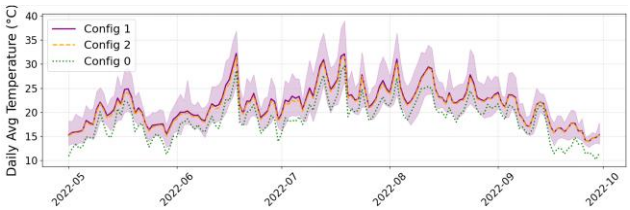

Figure 9 : Daily Average temperatures for Config 1, 2 and Config 0 (rural)

The two configurations yield remarkably similar results, with slight differences emerging towards the end of the day. Looking at the entire summer period (at least the one considered in our scenarios) both configurations also closely align. We can observe more precisely the UHI intensity differences between both models that differs depending on the hour of the day (Figure 10).

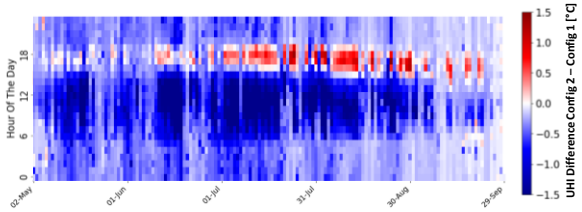

Figure 10: UHI Differences between Config 2 and Config 1 for summer (May 2 – September 30)

We show that the differences between the configurations are positive between 2PM and 6PM and negative otherwise, particularly between 6AM and 12PM. This aligns well with Figure 6, which demonstrated that the ray tracing method results in higher irradiances during this time of day.

The impact of these variations is further reflected in the cold degree days (CDD) presented in Table 7. This indicator represent the cumulative daily deviation from a reference temperature of **18°C** (Meteo France; Bhatnagar, Mathur, et Garg 2018). Here, the sum is calculated for the period from May 2 to September 30.

Table 7: CDD calculated for our 3 configurations

Configuration	CDD (°C.day)
Configuration 0 (rural)	297
Configuration 1	617
Configuration 2	571

We observe a twofold increase in CDD compared to the rural reference. The results between the two configurations show a difference of approximately 7%. This reduction can be attributed to the ray-tracing-based calculation of solar irradiance, which results in lower average daytime solar gains, particularly during the hottest hours, thereby limiting excessive heat accumulation.

These differences are also caused by the parameterization of UWG atmospheric model. The daytime boundary layer height is considerably underestimated compared to observations from the PANAME project, where it typically ranges between 1000 and 2000 meters and varies significantly through the day (Deardorff 1972; Hidalgo, Masson, et Gimeno 2010). A boundary layer of this height effectively traps heat during the day, creating an artificially pronounced urban heat island effect. A more detailed sensitivity analysis and optimization of the parameterization is a promising direction for future work, as is the integration of the influence of adjacent zones to the study area into the model.

4.3 Influence on energy cooling demand

The final step involves generating the BuildSysPro building models, using external air temperatures as boundary conditions provided either by the rural weather station (Configuration 0) the standard UWG code (Configuration 1), or our modified UWG version with detailed solar calculations (Configuration 2).

Cooling demands are analyzed using data calculated by BuildSysPro. The distribution of this cooling demand is reported on Figure 11 :

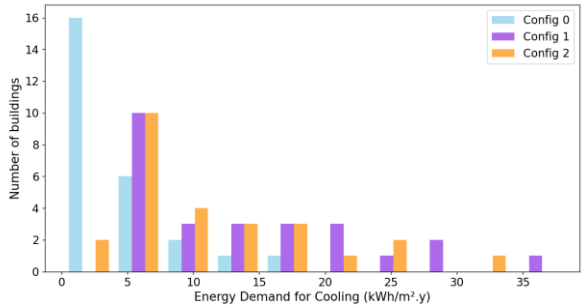

Figure 11: Distribution of the cooling demand for all configurations

https://doi.org/10.26868/25222708.2025.1153

In Table 8, we are giving the average cooling demand difference in percentage between Config 1 and 2

Table 8: Average cooling demands for all buildings

	Average cooling demand (kWh/m².y)
Configuration 0	4.26
Configuration 1	13.61
Configuration 2	11.61
2 vs 1 [%]	- 16.3 %

Moving from the Base configuration (Configuration 0) to Configuration 1 shows a clear urban heat island effect, with cooling demand increase. These changes are driven by the elevated urban air temperatures ($T_{out,urb}$) simulated by UWG. The cooling demand remains relatively low, attributed to the exclusively non-renovated building compositions and thus less efficient building envelopes (strong hypothesis). When transitioning from Config 1 to Config 2, the changes are more moderate, cooling demand decreasing (-16%). This reduction in cooling demand is likely due to more detailed ray-tracing calculations, which better account for shading, and building orientation. This trend is consistent with the CDD values (Table 7).

Finally, we can also compare the dynamic power curves over a few summer days: Figure 12 and Figure 13

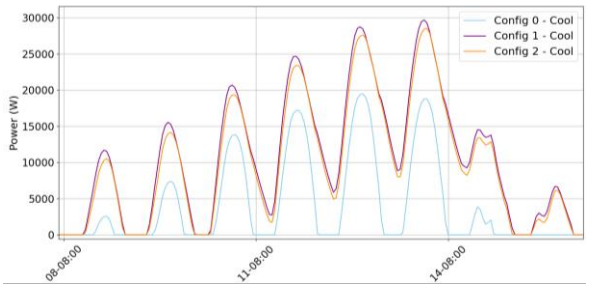

Figure 12: Cooling power for building 2, north-facing

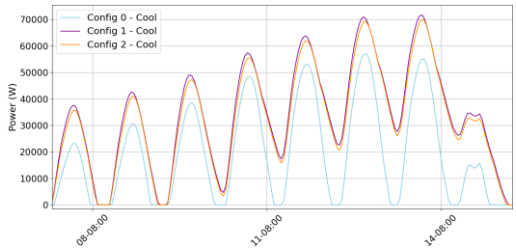

Figure 13: Cooling power for building 18, south-facing

We can draw the same conclusions as for the cumulative demand: the impact of the microclimate is clearly visible in the significantly higher power demands for Configurations 1 and 2. These demands peak at 5 PM, which aligns well with the occupancy scenarios used. Higher power demands are observed for Building 18, which faces south, making this observation consistent with expectations.

5 Conclusion

This study highlights the contribution of ray-tracing methods in refining urban microclimate modeling, particularly within the UWG framework. While the integration of detailed solar irradiance calculations provides a more accurate representation of solar irradiance on building walls and windows, the results in terms of air temperature remain broadly similar to those of the classic UWG model, with a change of RMSE around 0.2 °C.

The improved accuracy in simulating urban air temperatures with HelioBIM demonstrates its potential as a more reliable tool for urban energy modeling, particularly in dense urban environments. Furthermore, the present study focused on a homogeneous set of poorly insulated buildings during a summer period. In more diverse urban contexts—featuring heterogeneous morphologies, higher albedo surfaces, or extensive glazing—the benefits of advanced solar modeling could be more pronounced, as mean solar fluxes become less representative of local thermal conditions. Additionally, the model's sensitivity to key parameters, such as urban boundary layer height and surface exchange length scales, suggests that further optimization of these parameters could improve the accuracy of energy predictions.

Moreover, the results obtained for cooling demand are consistent with ranges reported in the literature. For instance, a study in southwestern Europe indicates that specific cooling energy needs can range from 1 to 90 kWh/m².year, depending on climate, urban density, and building characteristics (Zambito et al. 2022). Notably, Paris is cited in this study as one of the cities with relatively low cooling energy needs, with values often negligible and rarely exceeding 20 kWh/m².year, even in the most demanding configurations.

6 References

Bhatnagar, Mayank, Jyotirmay Mathur, et Vishal Garg. 2018. « Determining base temperature for heating and cooling degree-days for India ». *Journal of Building Engineering* 18 (juillet):270-80. https://doi.org/10.1016/j.jobe.2018.03.020.

Bocher, Erwan, Jérémy Bernard, Elisabeth Wiederhold, François Leconte, Gwendall Petit, Sylvain Palominos, et Camille Noûs. 2021. « GeoClimate: A Geospatial Processing Toolbox for Environmental and Climate Studies ». *Journal of Open Source Software* 6 (65): 3541. https://doi.org/10.21105/joss.03541.

Bocher, Erwan, Gwendall Petit, Jérémy Bernard, et Sylvain Palominos. 2018. « A geoprocessing framework to compute urban indicators: The MApUCE tools chain ». *Urban Climate* 24:153-74. https://doi.org/10.1016/j.uclim.2018.01.008.

Bouquerel, Mathias, Kevin Ruben Deutz, Benoît Charrier, Thierry Duforestel, Mickael Rousset, Bart Erich, Gerrit-Jan Van Riessen, et Thomas

Braun. 2021. « Application of MyBEM, a BIM to BEM Platform, to a Building Renovation Concept with Solar Harvesting Technologies ». In . https://doi.org/10.26868/25222708.2021.30153.

Bourquin, Léo, Mathias Bouquerel, Thierry Duforestel, & Emmanuel Bozonnet. 2024. « Intégration d'un modèle de microclimat méso-échelle dans une plateforme d'énergétique du bâtiment à l'échelle quartier », IBPSA France 2024.

Bozonnet, Emmanuel. s. d. « Impact des microclimats urbains sur la demande énergétique des bâtiments Cas de la rue canyon ».

Bueno, B., G. Pigeon, L. K. Norford, K. Zibouche, et C. Marchadier. 2012. « Development and Evaluation of a Building Energy Model Integrated in the TEB Scheme ». *Geoscientific Model Development* 5 (2): 433-48. https://doi.org/10.5194/gmd-5-433-2012.

Bueno, Bruno, Leslie Norford, Julia Hidalgo, et Grégoire Pigeon. 2013. « The Urban Weather Generator ». *Journal of Building Performance Simulation* 6 (4): 269-81. https://doi.org/10.1080/19401493.2012.718797.

Deardorff, James W. 1972. « Parameterization of the Planetary Boundary Layer for Use in General Circulation Models », février. https://journals.ametsoc.org/view/journals/mwre/100/2/1520-0493_1972_100_0093_potpbl_2_3_co_2.xml.

Hamdi, Hiba, Laure Roupioz, Thomas Corpetti, et Xavier Briottet. 2024. « Evaluation of the Urban Weather Generator on the City of Toulouse (France) ». *Applied Sciences* 14 (1): 185. https://doi.org/10.3390/app14010185.

Hidalgo, Julia, Valéry Masson, et Luis Gimeno. 2010. « Scaling the Daytime Urban Heat Island and Urban-Breeze Circulation ». *Journal of Applied Meteorology and Climatology* 49 (5): 889-901. https://doi.org/10.1175/2009JAMC2195.1.

Loga, Tobias, Britta Stein, et Nikolaus Diefenbach. 2016. « TABULA Building Typologies in 20 European Countries—Making Energy-Related Features of Residential Building Stocks Comparable ». *Energy and Buildings* 132 (novembre):4-12. https://doi.org/10.1016/j.enbuild.2016.06.094.

Mao, Jiachen, Joseph H. Yang, Afshin Afshari, et Leslie K. Norford. 2017. « Global Sensitivity Analysis of an Urban Microclimate System under Uncertainty: Design and Case Study ». *Building and Environment* 124 (novembre):153-70. https://doi.org/10.1016/j.buildenv.2017.08.011.

Martinez, S., A. Machard, A. Pellegrino, K. Touili, L. Servant, et E. Bozonnet. 2021. « A Practical Approach to the Evaluation of Local Urban Overheating– A Coastal City Case-Study ». *Energy and Buildings* 253 (décembre):111522. https://doi.org/10.1016/j.enbuild.2021.111522.

Masson, Valéry. 2000. « A Physically-Based Scheme For The Urban Energy Budget In Atmospheric Models ». *Boundary-Layer Meteorology* 94 (3): 357-97. https://doi.org/10.1023/A:1002463829265.

Meteo France. s. d. « Indice de rigueur - Degrés-jours unifiés aux niveaux national, régional et départemental ». Données et études statistiques pour le changement climatique, l'énergie, l'environnement, le logement et les transports. https://www.statistiques.developpement-durable.gouv.fr/indice-de-rigueur-degres-jours-unifies-aux-niveaux-national-regional-et-departemental.

Oke, T R. 1987. « Boundary Layer Climates, Second Edition ».

« PANAME – PAris region urbaN Atmospheric observations and models for Multidisciplinary rEsearch ». s. d. Consulté le 24 janvier 2025. https://paname.aeris-data.fr/.

Pérez-Lombard, Luis, José Ortiz, et Christine Pout. 2008. « A Review on Buildings Energy Consumption Information ». *Energy and Buildings* 40 (3): 394-98. https://doi.org/10.1016/j.enbuild.2007.03.007.

Plessis, Gilles, Aurelie Kaemmerlen, et Amy Lindsay. 2014. « BuildSysPro: A Modelica Library for Modelling Buildings and Energy Systems ». In , 1161-69. https://doi.org/10.3384/ecp140961161.

Santamouris, M. 2014. « Cooling the Cities – A Review of Reflective and Green Roof Mitigation Technologies to Fight Heat Island and Improve Comfort in Urban Environments ». *Solar Energy* 103 (mai):682-703. https://doi.org/10.1016/j.solener.2012.07.003.

Zambito, Andrea, Giovanni Pernigotto, Simon Pezzutto, et Andrea Gasparella. 2022. « Parametric Urban-Scale Analysis of Space Cooling Energy Needs and Potential Photovoltaic Integration in Residential Districts in South-West Europe ». *Sustainability* 14 (11): 6521. https://doi.org/10.3390/su14116521.